Asian Journal of Chemistry; Vol. 35, No. 11 (2023), 2759-2766

ASIAN JOURNAL OF CHEMISTRY

https://doi.org/10.14233/ajchem.2023.29070

Removal of Arsenic by Adsorption using Activated Carbon Derived from *Zea mays*

S. SURESH KUMAR[1], MALATHI CHALLA[1,*], P. MURALI KRISHNA[1] and P.R. DEEPTHI[2]

[1]Department of Chemistry, Ramaiah Institute of Technology (Autonomous Institute, Affiliated to Visvesvaraya Technological University, Belagavi), Bengaluru-560054, India
[2]Department of Physics, School of Engineering, Presidency University, Bengaluru-560065, India

*Corresponding author: E-mail: maalathichalla@msrit.edu

Received: 21 August 2023; *Accepted*: 27 September 2023; *Published online*: 31 October 2023; AJC-21433

The toxic pollutant arsenic ions present in the soil and water induce severe environmental and health issues in the North East of India and most of the Asian countries. This demand exploring the adsorption of arsenic ions in an aqueous medium by using a low-cost and non-pollutant adsorbent that is activated carbon obtained from the *Poaceae* family species (*Zea mays*). Activated carbon with calcium oxide (CaO) has been synthesized by pyrolysis at 650 ºC in the inert atmosphere. The characterization of activated carbon was done using a powder X-ray diffractometer, Fourier scanning electronic microscope, energy dispersive X-ray analysis and an inductively coupled plasma-mass spectrometer. The adsorption mechanism and efficacy of activated carbon were explored under optimized parameters such as pH of 5, 1 mg/mL of activated carbon dosage and 10 ppm of As(III) ions concentration at ambient temperature. The adsorption capacity of the activated carbon from the non-linear Sips model was found to be 8.4 mg/g and the linear Langmuir model was 29.85 mg/g. The adsorption mechanism from the non-linear, linear kinetic studies and Web Morris intraparticle diffusion model suggested the adsorption of arsenic ions by mass transfer, a diffusion mechanism as well as pseudo-second-order kinetics. Based on the results of desorption experiments, it is possible that the adsorbent can be reused for adsorption process for two cycles.

Keywords: *Poaceae* species, Pyrolysis, Activated carbon, As(III) ions, Adsorption, Desorption.

INTRODUCTION

Metals are generally extracted from their ores and also found in rocks when washed by groundwater or surface water. Metals in their ionic state are more stable and found in the Earth's crust with the variation of their concentration from place to place [1]. Various metals play a prominent role in science and technology due to their high electrical conductivity, brilliance and malleability. Metal ions, including manganese, iron, zinc, copper, *etc*. are necessary for human beings in specific amounts, however, when present in higher concentrations, these ions can become poisonous. The metals Hg, Cd, Pb and As have been categorized as highly toxic metal ions due to their carcinogenic nature even in low concentrations. The toxic nature of the metal will decide whether their existence in ppm or ppb levels in the soil and water bodies is safe for living organisms or not. Moreover, metal ions accumulate in the soil and water causing them to enter the plants either damaging or transforming into animals and humans. The first category toxic element arsenic is a metalloid existing in nature as it ores like arsenopyrite, orpiment, *etc.* It enters the environment *via* natural processes like weathering of rock and volcanic eruptions and *via* anthropogenic actions like industrial activities for example mining, smelting ore and agricultural activities like fertilizers, pesticides, insecticides, *etc.* However, it contaminates soil and water. The literature survey reveals that in South and Southeast Asia in the Asia continent, West Bengal, Tripura, Assam states and the basin of Ganga-Brahmaputra-Meghna river in India, the whole of Bangladesh nation suffers from arsenic poisoning that threatens the lifestyle of millions of people [2].

In general, arsenic exists in both inorganic and organic compounds. Inorganic arsenic form is more toxic and available in the form of H_2AsO_3 H_3AsO_3 with As(III) oxidation number and H_3AsO_4, $H_2AsO_4^-$, $HAsO_4^-$, AsO_4^{3-} contain As(V) oxidation number. Relatively, the solubility of As(III) is higher at 67-99% and its mobility is high which leads to easy contamination of the groundwater. According to the World Health Organization (WHO), the permissible limit of As(III) is 10 ppb with respect

to being more prominent in an anoxic environment and oxic environment arsenic is As(V) oxidation state [3-5]. More than 100 million people in the world are consuming arsenic-contaminated water that contains more than the threshold limit of arsenic. The toxicity of As(III) is 30-70 times more than As(V) as As(III) interacts with thiol (–SH) groups of enzymes and inhibits enzyme action, ATP synthesis with replacement of the phosphate group, gastrointestinal problems, anaemia, skin cancer/skin diseases and neurological defects [6].

There are many physical, chemical, phytoremediation and biological methods available to remove toxic arsenic compounds [7,8]. Among these, the adsorption of arsenic on the adsorbent is the most prominent low-cost and minimal-time consumption method. In literature, many nano-adsorbents like iron oxide, titanium oxide, *etc*. been used to remove toxic chemicals but these are associated with the disposal problem since they themselves cause toxicity at high concentrations [9]. In such adverse situations, biochar and its activated carbon are synthesized from the various parts of the plants used as the adsorbents [10,11]. Meanwhile, commercial activated carbon, carbon synthesized from rice husk, date pits, sugarcane waste, orange peel, coir pith, banana pith, cotton waste, sawdust, *etc.* used as effective adsorbents. Activated carbon used as the adsorbent is more in vogue and its inclination of performance depends upon its precursor, activation agent and the process of the activation.

With zinc chloride thermal activation of carbonized sample obtained from the *Dialium guineense* seed shell has shown an adsorption capacity of 47.08 mg/g [4-6,12,13]. Similarly, pristine biochar without and with surface modification using Fe, Fe with Mn have exhibited the adsorption capacity as 1FeC > $1Fe_2MnC$ > PB in pH of 7 at 298 K. In the same manner, good adsorption of arsenic ions has been observed on activated carbon surfaces modified with iron or cerium compounds due to chemi-sorption including physisorption [14]. Activated carbon without surface modification is more beneficial to use for the adsorption of toxic metal ions by taking into account the cost, minimal sludge production, eco-friendly and no disposal problem than the surface-modified activated carbon [12-15]. In light of above consideration and the part of ongoing work, it is worthwhile to synthesize activated carbon from the Poaceae family species (*Zea mays*) has been selected for the effective adsorption of arsenic ions in an aqueous medium.

EXPERIMENTAL

Chemicals of analytical grade (≥99%) from Sigma-Aldrich were purchased and used without further purification. Arsenic [P. No: NIST3103A] (NIST: National Institute of Science and Technology) from Sigma-Aldrich was purchased and taken as an aliquot quantity to get 10 ppm (diluted in 0.001 N HNO_3) in the aqueous medium to carry out the experiments.

Instrumentation: Activated carbon was characterized by Powder X-ray diffractometer (Philips PW1050 X-pert diffractometer with a Cu*K*α (λ = 1.5406 Å) radiation at 40 kV and 25 mA). Morphology of activated carbon was investigated by scanning electron microscopy (SEM) and energy dispersive X-ray analysis (EDX) using JEOL version JSM-6390LV. BET studies were carried out by Lab RAM HR and NOVA Touch LX. Thermo-Fisher, iCAP model of inductively coupled plasma-mass spectrometry (ICP-MS) was employed to measure arsenic ions in micrograms.

Synthesis of activated carbon: The roots of *Zea mays* were collected, cleaned, cut down to small pieces and dehydrated at 105-110 ºC for 2 days. Pulverization and ground of the roots were done to get a fine powder which was further subjected to pyrolysis at 600 ± 50 ºC in the presence of calcium oxide for 30 min under a nitrogen flow of 100 mL/min [12-14].

Adsorption studies: Adsorption experiments were explored to optimize the parameters like pH (2-10), dosage of activated carbon (10-150 mg), arsenic (As^{3+}) ions concentration (1-15 ppm) and time effect (0-90 min). The adsorption mechanism and capacity of the adsorbent were investigated by using 1000 mg/L of AC with 10 ppm of arsenic ions in the aqueous solution with a stirring rate of 600 rpm at a pH of 6, for 90 min [15,16]. An aliquot quantity of sample was collected and centrifuged to measure the left arsenic ions by ICP-MS in the subsequent intervals and calculated the removal percentage and the amount of arsenic ions adsorbed on the activated carbon surface at the specified time and the equilibrium using eqns. 1-3 [14].

$$\text{Removal efficiency } (\%) = \frac{C_o - C_e}{C_o} \times 100 \quad (1)$$

$$q_t = \frac{(C_o - C_t)}{m} \times V \quad (2)$$

$$q_e = \frac{C_o - C_e}{m} \times V \quad (3)$$

where C_o (mg/L) and C_t (mg/L) are the initial dye concentration and the dye concentration at any time, t, respectively. C_e (mg/L) is the dye concentration at equilibrium, q_e (mg/g) at an equilibrium, V (L) is the volume of the adsorbate and m (g) is the mass of adsorbent.

Analysis of linear and non-linear models: Linear regression models are the feasible tools to identify the best fitting model and quantify adsorbate distribution, analyzing the adsorption system and its consistency with the theoretical assumptions. The generally assessed method of linear regression to find out the suitability of the model is R^2, intercept and slope of the graph. Linear equations are transformations of non-linear equations that show poor linearity instead of high linear regression coefficients. For these reasons, the non-linear regression model which is the original robust calculation used to determine the adsorption model parameters. In non-linear models, the fit model is assessed by the error functions. The minimal error of the different kinds of error functions has been normalized implying the best overall fit model. An average of duplicate batch studies for adsorption of non-linear isotherms and kinetic data was computed by the solver tool Microsoft Excel® 2019 version. The regression coefficient (R^2), residual sum of square (RSS) and Chi^2 were calculated from the below equations [12]:

$$R^2 \frac{\Sigma(q_{e,pre,i} - q_{e,exp,avg})^2}{\Sigma(q_{e,pre,i} - q_{e,exp,avg})^2 - \Sigma(q_{e,pre,i} - q_{e,exp,i})^2} \quad (4)$$

$$RSS = \sum_{i=1}^{N} (q_{e,exp,i} - q_{e,pre,i})^2 \quad (5)$$

$$\chi^2 = \sum_{i=1}^{N} \frac{(q_{e,exp} - q_{e,pre})^2}{q_{e,exp}} \quad (6)$$

RESULTS AND DISCUSSION

The activated carbon synthesized from the Poaceae family species (*Zea mays*) has been characterized by several analytical techniques.

PXRD studies: Fig. 1 exhibits the PXRD of activated carbon before adsorption (ACB) and after adsorption of arsenic ions (ACA). The diffractogram of activated carbon with uneven peaks and orientations revealed both the crystalline phase and amorphous phase. The crystalline nature of activated carbon was decreased after As(III) ion adsorption. The method of synthesis of carbon and its activation plays a role in the crystallinity. The orthorhombic crystalline peaks that appeared at 2θ 26.61°, 43.45°, 46.32°, 54.81° and 56.68° are relevant to (111), (100), (110), (222) and (211) planes, respectively [5,6,12-16].

Field scanning electron microscopy/energy-dispersive X-ray spectrometric (FSEM-EDX) studies: The morphology with the surface state of the activated carbon was evaluated from SEM images. The SEM images (Fig. 2) revealed that the average particle size of the carbon particles was found to be 395.86 nm. The images revealed that activated carbon has a slight amorphous phase. The EDX data indicates the presence of carbon, oxygen, silicon, calcium and potassium in weight percentages as 79.78, 16.29, 0.55, 2.25 and 1.21%, respectively. The EDX spectrum pronounces that Ca which was used in the

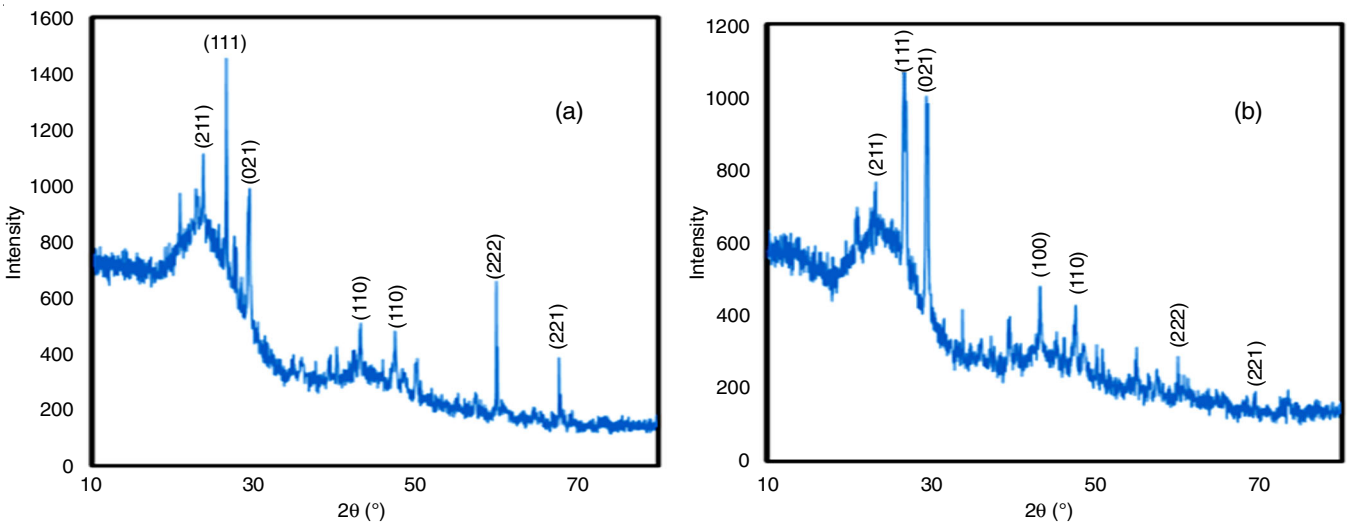

Fig. 1. PXRD of activated carbon of (a) before adsorption of As(III) ions, (b) after adsorption of As(III) ions

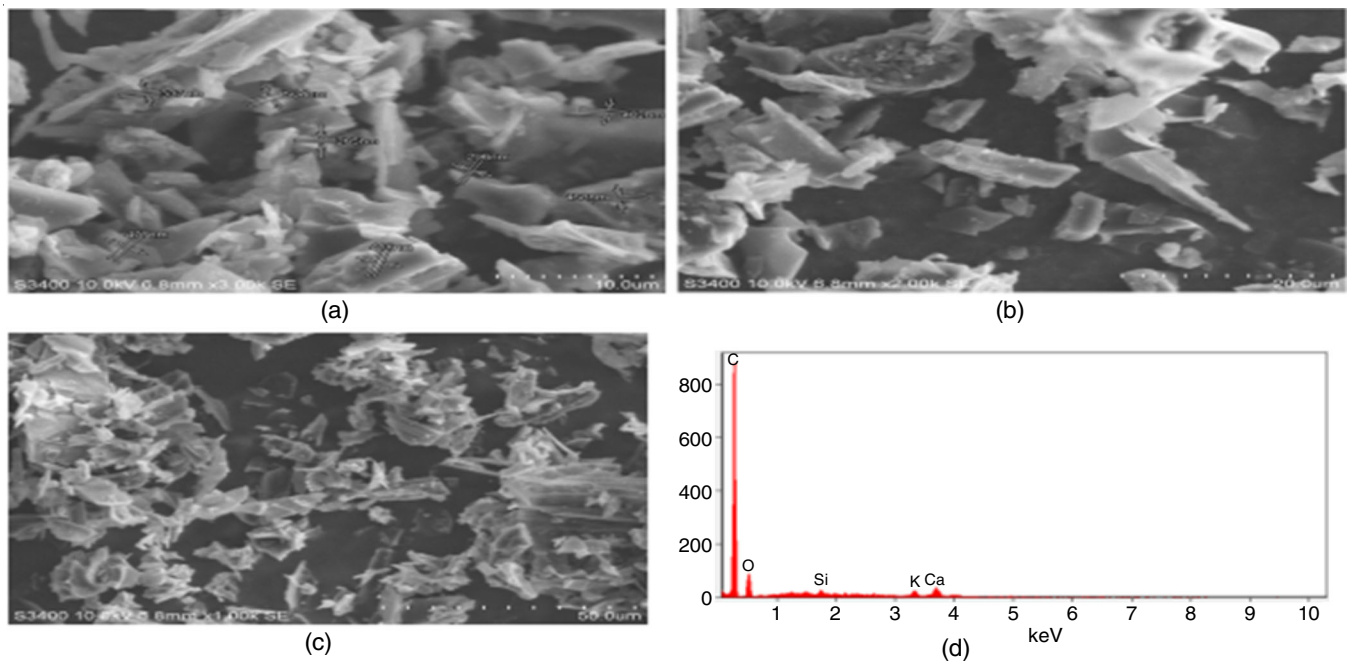

Fig. 2. FSEM-EDX images of activated carbon before adsorption of arsenic ions (a) 10 µm magnification (b) 20 µm magnification, (c) 50 µm magnification, (d) energy dispersive X-ray spectrum of activated carbon

activation process, exists in the activated carbon. The existence of K and Si in activated carbon may be due to the soil structure where the maize was grown [15-17]. The presence of elements in the activated carbon is shown in Table-1.

TABLE-1
PRESENCE OF ELEMENTS WITH WEIGHT (%) AND ATOMIC (%) IN ACTIVATED CARBON

Element	Weight (%)	Atom (%)	Error
C	79.78	85.58	± 1.19
O	16.20	13.05	± 1.95
Si	0.55	0.25	± 0.09
Ca	2.25	0.72	± 0.32
K	1.21	0.40	± 0.12

BET studies: The analysis of BET was conducted at 77 K and 93.961 kPa in a saturated N_2 atmosphere disclosing surface area and pore size with the volume related to the adsorbent. Fig. 3 reveals type II isotherm according to the IUPAC classification. BET surface area was 422 m^2/g, mean pore diameter 8.191 nm and total pore volume 0.173 cm^3/g and considered a mesoporous structure [12].

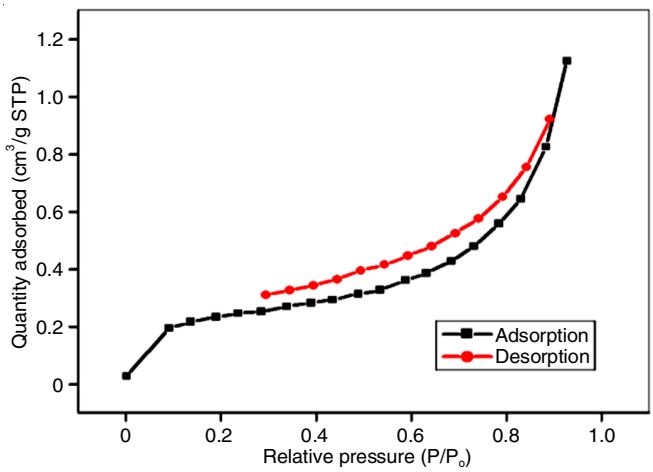

Fig. 3. Plot of N_2 adsorption and desorption studies

Adsorption studies

Optimization of the adsorption parameters: Adsorption studies of the prepared activated carbon were carried out by optimizing the following parameters.

pH effect: The pH parameter effectively influences the adsorption process *via* regulating either electrostatic repulsion or attraction of metal ions on the adsorbent surface. For this, arsenic ions adsorption on activated carbon has been systematically examined from pH of 2 to 10, which is displayed in Fig. 4a. The high removal percentage of arsenic ions was at a pH of 5 than in the alkaline pH so that pH of 5 was optimized for exploration of arsenic ions' adsorption. The grappling of H^+ over As(III) ions in the aqueous phase on the negatively charged activated carbon surface causes minimal adsorption of As(III) ions at lower pH. At higher pH, Na^+ ions competed with arsenic(III) ions resulting in low adsorption [18,19].

Adsorbent dosage: Another parameter that influences the adsorption capacity of activated carbon is the dosage effect. This was investigated by adding from 10 mg to 150 mg of

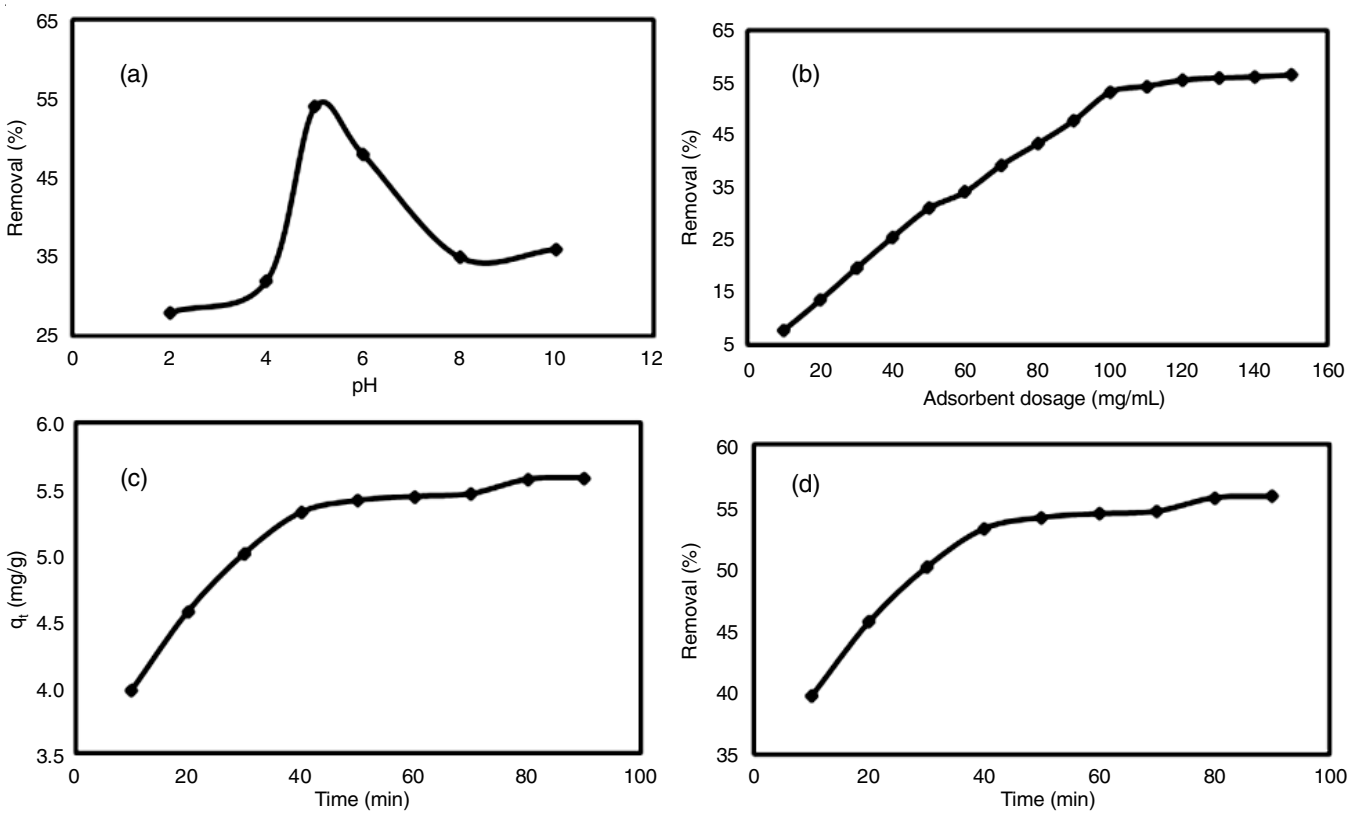

Fig. 4. Optimization of parameters for As(III) ions adsorption on activated carbon (a) pH effect, (b) adsorbent dosage effect, (c) amount of arsenic ions adsorption and (d) time effect

activated carbon dosage in 100 mL of 10 ppm of aqueous As(III) ions solution. It is observed that there is a linearity in the uptake As(III) adsorption up to 100 mg of activated carbon dosage as displayed in Fig. 4b and further saturation is attained because the congregation of adsorbent particles in the high dosage reduces the surface area including the active sites. So, 100 mg of activated carbon is optimized for the adsorption of As(III) ions.

Time effect: The other parameter is the time effect which was studied from 10-90 min to explore the efficiency of the adsorption process. The arsenic(III) adsorption enhanced with subsequent time intervals increased upto 60 min, as caused by the interaction between As(III) ions and the surface of activated carbon. The maximum amount of As(III) ions adsorption has been 5.58 mg/g (Fig. 4c). Further, a saturation of adsorption happened due to the equilibrium established (Fig. 4d).

Adsorption kinetic studies: To illustrate the reaction pathway between adsorbate As(III) ions and adsorbent activated carbon and the mechanism of the adsorption process, the linear and non-linear kinetic models have been employed. Largergen pseudo-first-order kinetic model explains the adsorption rate on the basis of surface active sites through diffusion and boundary layer effect [19-22]. The non-linear pseudo-first-order kinetic model is given below in eqn. 7 and its linear form in eqn. 8:

$$q_t = q_e(1 - e^{-k_1 t}) \quad (7)$$

$$\log(q_e - q_t) = \ln q_e - k_1 t \quad (8)$$

where q_t is the amount adsorbed at time t (mg/g) and q_e is the adsorption capacity at equilibrium (mg/g). In addition, k_1 is the pseudo-first-order rate coefficient (min^{-1}).

The pseudo-second-order kinetic model describes the adsorption process through chemisorption. The non-linear and linear equations of pseudo-second-order (PSO) and intraparticle diffusion (IPD) are mentioned in the below eqns. 9 & 10 [21-24]:

$$q_t = \frac{k_2 q_e^2 t}{1 + k_2 q_e t} \quad (9)$$

$$\frac{t}{q_t} = \frac{1}{k_2 q_e^2} + \frac{1}{q_e} t \quad (10)$$

where k_2 is the pseudo-second-order rate coefficient (mg g^{-1} min^{-1}), q_e is the amount of adsorbate at the equilibrium and q_t is the amount of adsorbate at a given time.

$$q_t = k_d t^{1/2} + C \quad (11)$$

where C is the intercept, a constant represents the boundary layer effect and k_{id} (mol g^{-1} $min^{0.5}$) is the intraparticle diffusion rate.

The linear trend of the pseudo-first-order model (PFO) in its linear form is apparently not fit to explain As(III) ions adsorption on activated carbon by considering poor linearity with a low linear regression coefficient. Although linear results in Table-2 are not recommended for the pseudo-first-order model whereas the non-linear pseudo first order model is in agreement with the experimental data with the consideration of R^2, RSS and Chi^2 were 0.999, 2.386 and 0.4636 (Table-3), respectively. In fact, the pseudo-second order (PSO) model depends on many factors such as the initial adsorbate concentration, pH adsorbent, particle size, dose and nature of adsorbate. The linear and non-linear form of the pseudo seconder model has exhibited good agreement by insight into the parameters mentioned in Tables 2 and 3. Overall, the comparison of R^2 values of PFO and PSO are the same but the statistical parameters RSS and Chi^2 values (Table-3) of the pseudo-second-order model were very low error than the pseudo-first-order model [21]. The amount of arsenic ions adsorbed at equilibrium (q_e) was 5.148 mg/g and 5.07 mg/g for PFO and PSO models, respectively.

Apart from this, the intraparticle diffusion model plot in Fig. 5b suggests that the adsorption mechanism is a multistep process [21-24]. The linear part at the initial stage is due to film diffusion on the available surface active site; the curve part (stage II) is caused by the percolation of As(III) ions through the adsorbent pores and the plateau (stage III) declares saturation of the adsorbent surface leads to attaining equilibrium state. The increase of C values (Table-4) as 2.62, 3.65 and 4.84 for the stages I, II and III, respectively and minimized K_d values with time (0.4650, 0.2527, 0.0762 for the stages I, II and III, respectively) proves that the rate of adsorption is high at the initial stage and further reduces because of the enhancement of diffusional resistance and increase of boundary layer effect [12,21-25]. Summarizing the kinetic models for the adsorption mechanism, the rate-limiting step of the adsorption mechanism is explained by the best-fit model pseudo-second-order and intraparticle diffusion models.

Adsorption isotherms: The influence of the initial concentration of As(III) ions on the adsorption capacity of the adsorbent was examined by the linear and non-linear isotherms.

TABLE-2
LINEAR KINETIC MODELS' PARAMETERS

Kinetic models	Linear equation	R^2	Kinetic constant	q_{epre} (mg/g)
Pseudo first-order (PFO)	y = -0.0156x + 0.00462	0.8342	(k_1) 2.6×10^{-4} min^{-1}	-5.377
Pseudo second-order (PSO)	y = 0.0180x + 0.0867	0.9914	(k_2) 3.73×10^{-3} g mg^{-1} min^{-1}	55.55

TABLE-3
NON-LINEAR KINETIC MODELS' PARAMETERS

Kinetic models	Kinetic parameters		Statistical parameters		
Pseudo first-order (PFO)	K_1 (1/min)	q_e (mg/g)	R^2	RSS	χ^2 (Chi)
	4.89	5.148	0.9999	2.386	0.4636
Pseudo second-order (PSO)	K_2 (mg g^{-1} min^{-1})	q_e (mg/g)	R^2	RSS	χ^2 (Chi)
	0.0329	5.907	0.9999	0.0356	0.0068

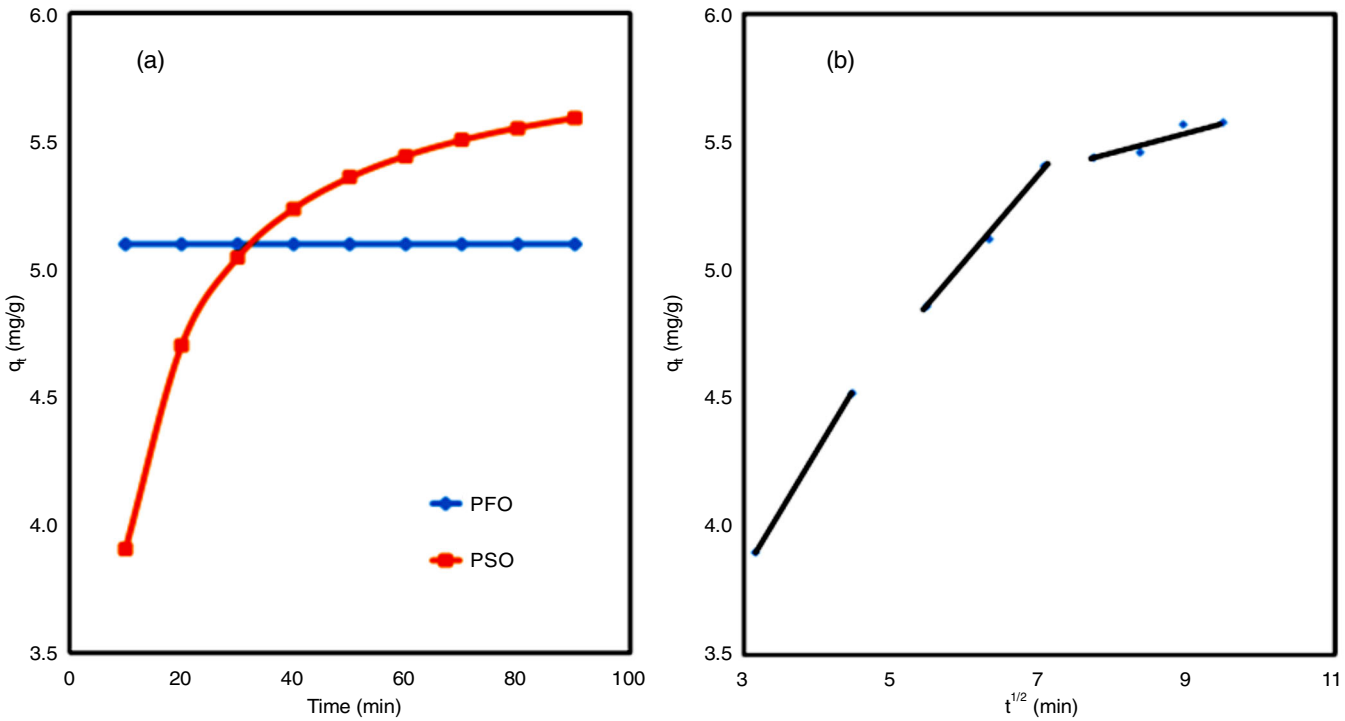

Fig. 5. Non-linear plots of arsenic ions' adsorption on activated carbon, (a) Kinetic models and (b) IPD model

TABLE-4
WEB-MORRIS INTRAPARTICLE DIFFUSION MODELS

IPD	K_d (mg g^{-1} $min^{-0.5}$)	C (mg/g)	R^2
Stage I	0.4650	2.52	1.000
Stage II	0.2527	3.65	0.9635
Stage III	0.0762	4.84	0.9860

Langmuir model describes monolayer adsorption with a finite number of specific active sites without steric hindrance and lateral interaction between adsorbate and the adsorbent. The non-linear and linear equations of the Langmuir isotherm models are given in eqns. 12 and 13, respectively [21].

$$q_e = \frac{q_m K_L C_e}{1 + K_L C_e} \quad (12)$$

$$\frac{C_e}{q_e} = \frac{1}{K_L q_m} + \frac{C_e}{q_m} \quad (13)$$

The calculation of separation factor (R_L) from the Langmuir model is given below eqn. 14. The R_L value always lies between 0 to 1. More interestingly, the $R_L = 0$ process is irreversible, if $R_L = 1$ it is linear and if $R_L > 1$ it is unfavourable.

$$R_L = \frac{1}{1 + (K_L C_o)} \quad (14)$$

where R_L is the separation factor, C_e is the concentration of adsorbate at equilibrium, C_o is the initial concentration of adsorbate, q_e (mg/g) is the amount of adsorbate at equilibrium, q_m is the maximum amount of adsorbate, K_L is the Langmuir constant.

Freundlich isotherm model accounts for the multilayer adsorption *via* no uniform distribution of adsorption heat over heterogeneous surface. The non-linear and its linear equations are given below in eqns. 15 and 16, respectively [26].

$$q_e = K_F C_e^{1/n} \quad (15)$$

$$\ln q_e = \frac{1}{n} \ln C_e + \ln K_F \quad (16)$$

where K_F is the Langmuir and Freundlich constants, C_e is the concentration of adsorbate at equilibrium, q_e (mg/g) is the amount of adsorbate at equilibrium, 1/n is the intensity of adsorption; 1/n = 0, irreversible, 1/n > 1, unfavourable and 0 < 1/n < 1, is favourable between adsorbent and absorbate.

The three-parameters non-linear and linear Sips model (eqns. 17 and 18) is the combination of the Langmuir and Freundlich models which depends on pH, temperature and concentration of adsorbate. This model refers to adsorption on the heterogenous surface without limiting the concentration of adsorbate in the medium. Thus, it simplifies to Freundlich model in the low concentration of the adsorbate whereas it reduces to the Langmuir model at the high concentration of the adsorbate.

$$q_e = \frac{q_m K_s C_e^{n_s}}{1 + K_s C_e^{n_s}} \quad (17)$$

$$\ln\left(\frac{q_e}{q_m - q_e}\right) = \frac{1}{n_s} \ln C_e + \ln K_s \quad (18)$$

where K_s (L/mg) is the Sips equilibrium constant, q_s (mg/g) is the specific adsorption capacity at saturation and n_s index of heterogeneity proposes the adsorption process; at high adsorbate concentration ($n_s = 1$), the equation follows Langmuir's monolayer adsorption, while at low adsorbate concentration ($n_s = 0$), the equation follows Freundlich adsorption.

The R^2 values of linear regression of the Langmuir, Freundlich and Sips models were 0.9987, 0.9749 and 0.8589, respectively. So, the linear equations of the isotherm models and R^2 (Table-5) suggest the Langmuir model is suitable.

The maximum adsorption capacity of As(III) ions from the Langmuir linear model was found to be 29.85 mg/g (Table-5). In the non-linear regression models, Langmuir and Freundlich's models have exhibited almost the same R^2, RSS and Chi^2 values but the constant $K_L < K_F$ and adsorption capacity from the Langmuir model (q_L) is very high value to the experimental value [21,26,27]. For this reason, the three parameters Sips model which is a combination of the Langmuir and Freundlich models, is employed to investigate the adsorption capacity of activated carbon [25-29]. The evaluated n_s value of the Sips model is greater than 1 which recommends adsorption is favourable at high concentrations. By considering the data in Table-6, the R^2 and the least error of RSS and chi^2 also envisage the best-fit model is the Sips model. The predicted q_e (mg/g) value from the Sips model is much closer to the experimental value [30-35]. Therefore, the adsorption capacity of activated carbon for arsenic ions was found to be 8.314 mg/g. Thus, based on the non-linear models, the adsorption of As(III) is favourable at higher concentrations with the least error of statistical parameters from the best-fit Sips model but linear models pronounced the Langmuir model which is mono-layer chemisorption [20,25]. Furthermore, it is envisaged by the pseudo-second-order kinetic model by both linear and non-linear regression analysis.

Comparitive studies: From Table-7, it is observed that the required dosage of activated carbon in the present study is 3 times less than the activated carbon from *Tamarix* leaves and the adsorption capacity for As(III) is almost the same value. Also, activated carbon obtained from *Cassia tora* has shown poor adsorption with more time consumption (140 min) than in the present study. The commercial activated carbon with metal oxides has exhibited a little more adsorption but the equilibrium time was more. Overall, the conclusion is that activated carbon from *Zea mays* roots has good adsorption capacity and its surface modification may improve its efficiency.

Desorption studies: Desorption studies have also been performed using hot water containing 0.001 N at the same experimental conditions. The desorption of As(III) ions was much less around 25% of its adsorption amount in the first cycle, 10 % in the second cycle and 3% only in the third usage due to quasi-chemical bonds between the adsorbate and adsorbent [32-35]. From these studies, activated carbon may be used around two times only.

TABLE-5
LINEAR ISOTHERM MODELS' PARAMETERS

Isotherm models	Linear equation	R^2	Isotherm constant
Langmuir	y = 0.6830x + 0.0335	0.9987	K_L = 0.049 (Lg^{-1}); q_m = 29.85 (mg/g)
Freudlich	y = 0.8629x + 0.3569	0.9749	K_F = 0.357 (Lmg^{-1}); 1/n = 0.8629
Sips	y = 2.1349x – 1.435	0.8589	K_S = -0.361; n_s = 0.468

TABLE-6
NON-LINEAR ISOTHERM MODELS' PARAMETERS AND STATISTICAL PARAMETERS

Isotherm models	Non-linear parameters			Statistical parameters		
Langmuir	R_L	q_L (mg/g)	K_L (Lg^{-1})	R^2	RSS	χ^2 (Chi)
	0.998	4049.2	0.00027	0.9965	12.628	2.9464
Freundlich	1/n	K_F (L mg^{-1})		R^2	RSS	χ^2 (Chi)
	0.238	4.509		0.9965	12.692	2.9610
Sips	n_s	q_s (mg/g)	K_s (L/mg)	R^2	RSS	χ^2 (Chi)
	1.721	8.314	0.156	0.9997	1.12	0.2596

TABLE-7
COMPARISON OF THE ADSORPTION CAPACITY OF ACTIVATED CARBON

Source for activated carbon	Modified surface	Surface area (m^2/g)	Optimization of the parameters				Adsorption capacity	Ref.
			pH	AC dosage (mg/mL)	Adsorbate conc. (ppm)	Time		
Dialiumguineense seed shell	$ZnCl_2$	533.94	6	4	100	25	47.08 (L)	[2]
Wood	$FeCl_3$ pyrolysis	181	9	2	1.0	1400	0.72 (L)	[4]
Used tea	Iron oxide	167	8	0.5	25	150	6.83 (L)	[6]
Commercial	$ZrOCl_2$, $MnSO_4$		10	0.4	30	1000	132.28 (L)	[14]
Sludge-biochar	$ZnCl_2$, $FeCl_3$	525	3	4.3	20	60	4.24 (L)	[15]
Cassia tora	Pyrolysis		8	1.2	1.0	140	26.62 (L)	[2]
Coal	Pyrolysis	1215	6	1.0	0.5	60	1.491 (L)	[3]
Tamarix leaves	Pyrolysis	252.3	7	3.0	10	40	37.3 (L)	[5]
Sugar cane	$FeCl_3$/$FeSO_4$	856, 803	7	0.15	0.6	20	0.148 (L)	[30]
Zea mays roots	Pyrolysis	422	5	1.0	10	60	29.85 (L) 8.34 (NL)	Present study

L: Linear regression models, NL: Non-linear regression models.

Conclusion

Activated carbon was obtained from the roots of *Zea mays* for the effective adsorption of arsenic(III) ions. The characterization studies revealed that the synthesized activated carbon is in both crystalline and amorphous phases. The adsorption capacity of activated carbon towards the removal efficiency of As(III) ions in aqueous solution reveals that activated carbon has arsenic adsorption of more than 50% and follows the pseudo-second-order model along with film diffusion and mass transfer mechanisms. The isotherm studies pronounced that the adsorption capacity of activated carbon for As(III) ions was around 8.34 mg/g by the non-linear regression Sips model but the Langmuir linear regression model showed the adsorption capacity of 29.85 mg/g for As(III) ions. From the desorption studies, it was found that activated carbon may be used twice. The uniqueness of the work is to improve the crystalline nature of activated carbon using the pyrolysis method and minimal work done to employ a non-linear regression model for As(III) adsorption on the activated carbon.

ACKNOWLEDGEMENTS

The authors are thankful to Visvesvaraya Technological University, Belagavi, India for the encouragement. The authors are also grateful to the Shri Ram Industrial Research Centre (SRI) and CAMT, Ramaiah Institute of Technology, Bengaluru, Karnataka, India for providing the research facilities.

CONFLICT OF INTEREST

The authors declare that there is no conflict of interests regarding the publication of this article.

REFERENCES

1. A. Sarkar, B. Paul and G.K. Darbha, *Chemosphere*, **299**, 134369 (2022); https://doi.org/10.1016/j.chemosphere.2022.134369
2. J.U. Ani, A.E. Ochonogor, K.G. Akpomie, C.S. Olikagu and C.C. Igboanugo, *SN Appl. Sci.*, **1**, 1304 (2019); https://doi.org/10.1007/s42452-019-1335-1
3. A.L. Srivastav, T.D. Pham, S.C. Izah, N. Singh and P.K. Singh, *Bull. Environ. Contam. Toxicol.*, **108**, 616 (2022); https://doi.org/10.1007/s00128-021-03374-6
4. C.K. Chen, J.J. Chen, N.T. Nguyen, T.-T. Le, N.-C. Nguyen and C.-T. Chang, *Sustain. Environ. Res.*, **31**, 29 (2021); https://doi.org/10.1186/s42834-021-00100-z
5. F. Wilson, P. Tremain and B. Moghtaderi, *Energy Fuels*, **32**, 4167 (2018); https://doi.org/10.1021/acs.energyfuels.7b03221
6. W.A.H. Altowayti, A.A. Salem, A.M. Al-Fakih, A. Bafaqeer, S. Shahir and H.A. Tajarudin, *Metals*, **12**, 1664 (2022); https://doi.org/10.3390/met12101664
7. K.T. Lim, M.Y. Shukor, H. Wasoh, *Biomed. Res. Int.*, **2014**, 503784 (2014); https://doi.org/10.1155/2014/503784
8. H. Pezeshki, M. Hashemi and S. Rajabi, *Heliyon*, **9**, e14246 (2023); https://doi.org/10.1016/j.heliyon.2023.e14246
9. M. Hashemi, S. Rajabi and S. Maleky, Toxicity and Health Impacts of Nanoadsorbents, In: Adsorption through Advanced Nanoscale Materials Applications in Environmental Remediation Micro and Nano Technologies, Elsevier, Chap. 7, pp. 461-482 (2023).
10. M. Geca, M. Wisniewska and P. Nowicki, *Adv. Colloid Interf. Sci.*, **305**, 102687 (2022); https://doi.org/10.1016/j.cis.2022.102687
11. P. Srivatsav, B.S. Bhargav, V. Shanmugasundaram, J. Arun, K.P. Gopinath and A. Bhatnagar, *Water*, **12**, 3561 (2020); https://doi.org/10.3390/w12123561
12. T. Mahmood, M. Aslam, A. Naeem, T. Siddique and S.U. Din, *J. Chil. Chem. Soc.*, **63**, 3855 (2018); https://doi.org/10.4067/s0717-97072018000103855
13. M. Challa, S. Chinnam, A.M. Rajanna, A. Nandagudi, B.C. Yallur and V. Adimule, *Heliyon*, **9**, e13223 (2023); https://doi.org/10.1016/j.heliyon.2023.e13223
14. S. Deshmukh, P.V. Thorat and N.S. Topare, *J. Catal. Catal.*, **5**, 15 (2018).
15. N. Sofyan, S. Alfaruq, A. Zulfia and A. Subhan, *J. Kimia dan Kemasan*, **40**, 9 (2018); https://doi.org/10.24817/jkk.v40i1.3767
16. E. Koohzad, D. Jafari and H. Esmaeili, *Chemistry Select*, **4**, 12356 (2019); https://doi.org/10.1002/slct.201903167
17. Y. Yin, T. Zhou, H. Luo, J. Geng, W. Yu and Z. Jiang, *Colloids Surf. A: Physicochem. Eng. Aspects*, **575**, 318 (2019); https://doi.org/10.1016/j.colsurfa.2019.04.093
18. Y. Yang, R. Zhang, S. Chen, J. Zhu, P. Wu, J. Huang and S. Qi, *RSC Adv.*, **12**, 7720 (2022); https://doi.org/10.1039/D1RA08941B
19. W. Zhang, Y. Cho, M. Vithanage, S.M. Shaheen, J. Rinklebe, D.S. Alessi, C.-H. Hou, Y. Hashimoto, P.A. Withana and Y.S. Ok, *Biochar*, **4**, 55 (2022); https://doi.org/10.1007/s42773-022-00181-y
20. T. Sumathi and G. Alagumuthu, *Chem. Sci. Rev. Lett.*, **11S**, 95 (2014).
21. A.E. Rodrigues and C. Manuel-Silva, *Chem. Eng. J.*, **306**, 1138 (2016); https://doi.org/10.1016/j.cej.2016.08.055
22. I.Y. Erwa, O.A. Ishag, O.A. Alrefaei and I.M. Hassan, *J. Turk. Chem. Soc.*, **9**, 67 (2022); https://doi.org/10.18596/jotcsa.904311
23. S. Yao, Z. Liu and Z. Shi, *J. Environ. Health Sci. Eng.*, **12**, 58 (2014); https://doi.org/10.1186/2052-336X-12-58
24. L. Tang, S. Zhang, G.-M. Zeng, Y. Zhang, G.-D. Yang, J. Chen, J.-J. Wang, J.-J. Wang, Y.-Y. Zhou and Y.-C. Deng, *J. Colloid Interface Sci.*, **445**, 1 (2015); https://doi.org/10.1016/j.jcis.2014.12.074
25. T.P.K. Murthy, B.S. Gowrishankar, R.H. Krishna, M.N. Chandraprabha and R.S. Rao, *Mater. Res. Express*, **6**, 055512 (2019); https://doi.org/10.1088/2053-1591/aafe3f
26. J. Lopez-Luna, L.E. Ramirez-Montes, S. Martinez-Vargas, A.I. Martínez, O.F. Mijangos-Ricardez, M.C.A. Gonzalez-Chavez, R. Carrillo-Gonzalez, F.A. Solis-Dominguez, M.C. Cuevas-Diaz and V. Vazquez-Hipolito, *SN Appl. Sci.*, **1**, 950 (2019); https://doi.org/10.1007/s42452-019-0977-3
27. E.E. Merodio-Morales, H.E. Reynel-Ávila, D.I. Mendoza-Castillo, C.J. Duran-Valle and A. Bonilla-Petriciolet, *Int. J. Environ. Sci. Technol.*, **17**, 115 (2020); https://doi.org/10.1007/s13762-019-02437-w
28. N. Tzabar and H.J.M. ter Brake, *Adsorption*, **22**, 901 (2016); https://doi.org/10.1007/s10450-016-9794-9
29. T.A. Saleh, M. Tuzen, A. Sarý and N. Altunay, *Chem. Eng. Res. Des.*, **183**, 181 (2022); https://doi.org/10.1016/j.cherd.2022.04.042
30. T.S. Singh and K.K. Pant, *Sep. Purif. Technol.*, **48**, 288 (2006); https://doi.org/10.1016/j.seppur.2005.07.035
31. D. Mohan, S. Markandeya, S.B. Dey, S.B. Dwivedi and S.P. Shukla, *Curr. Sci.*, **117**, 649 (2019); https://doi.org/10.18520/cs/v117/i4/649-661
32. L. Tang, S. Zhang, G.-M. Zeng, Y. Zhang, G.-D. Yang, J. Chen, J.-J. Wang, J.-J. Wang, Y.-Y. Zhou and Y.-C. Deng, *J. Colloid Interface Sci.*, **445**, 1 (2015); https://doi.org/10.1016/j.jcis.2014.12.074
33. A. Pholosi, E.B. Naidoo and A.E. Ofomaja, *S. Afr. J. Chem. Eng.*, **32**, 39 (2020); https://doi.org/10.1016/j.sajce.2020.01.005
34. D. Picón, N. Torasso, J.R.V. Baudrit, S. Cerveny and S. Goyanes, *Chem. Eng. Res. Des.*, **185**, 108 (2022); https://doi.org/10.1016/j.cherd.2022.06.042
35. V.O. Njoku, M.A. Islam, M. Asif and B.H. Hameed, *J. Anal. Appl. Pyrolysis*, **110**, 172 (2014); https://doi.org/10.1016/j.jaap.2014.08.020